FLOW AROUND A CYLINDER SWIMMING IN A QUIESCENT FLUID

M. Nazarinia*, D. Lo Jacono, M. C. Thompson and J. Sheridan
Department of Mechanical & Aerospace Engineering, Monash University, Australia

ABSTRACT. The flow structures around a circular cylinder undergoing combined oscillatory translation and rotation in a quiescent fluid have been investigated experimentally and numerically. Experiments were performed for the set of parameters that was shown previously to result in a net thrust i.e. the *swimming cylinder* case. The range of Reynolds number covered in this study was $141 \leq Re \leq 628$. The velocity fields were measured in multiple planes using particle image velocimetry. The experimental setup was such that the cylinder was mounted vertically to an actuator to create the horizontal translation. The circular cylinder used has an outer diameter of 20mm and length of 800mm. Experimental results confirmed that at certain phase differences between the two motions, i.e. out-of-phase or in phase, the cylinder is capable of generating thrust in a perpendicular direction to the translational oscillation. Experiments were also undertaken to investigate the three-dimensional nature of the flow. Additional analysis on the stability of such flow has been carried out with numerical simulation and confirmed the experimental measurements.

Keywords: *wake, cylinder, quiescent, instability*

INTRODUCTION

A circular cylinder undergoing a combination of translation and rotation oscillatory motions in quiescent fluid has not received much attention until now. It is well known that when a bluff body is oscillating translationally in a quiescent fluid, secondary streaming is generated around the body owing to the influence of nonlinear effects [1]. However, the combination of the two oscillatory forcing mechanisms can, under specific conditions, result in a net thrust being experienced by the circular cylinder in a direction normal to the translational axis [2]. The cylinder experiencing thrust and undergoing a series of pitch and plunge motions has been labeled the *swimming cylinder*. Numerous studies of flow over bodies undergoing pure oscillatory motions exist in the literature. These oscillatory motions include pure translation [3-8] and pure rotation [9-11].

So far, to the best knowledge of the authors, only the investigation by Blackburn et al. [2] and several more recent ones [12-14] have been reported on the combined oscillatory motion. However, the work by Blackburn et al. [2] is the only one on the swimming cylinder (e.g. the quiescent case) and to date no experiments have confirmed this phenomenon. A number of interesting features have been shown to occur as a result of combining the two motions. Blackburn et al. [2] found out that a jet flow will be produced by the cylinder when the two imposed motions are in phase or of opposite phases, i.e. $\Phi = (0, \pi)$. The propulsive force produced by the cylinder caused it to accelerate until eventually reaching a terminal speed of 33% of the peak translational speed.

* Corresponding author: Mr. M. Nazarinia
Phone: + (61)-3-99053537, Fax: + (61)-3-99051825
E-mail address: mehdi.nazarinia@monash.edu.au

The purpose of the present study is to investigate not only the near wake structures arising from this combination of forcing mechanisms, but also their associated three-dimensional nature, which has not received attention so far. The present study incorporates experimental and numerical results. To characterise the experiments, the authors employed particle image velocimetry (PIV) technique. A direct numerical simulation and Floquet analysis are also used to support and extend the present investigation. After defining the problem and the methods and techniques used, the results and discussion will be presented below.

PROBLEM DEFINITION

The flow over a cylinder undergoing combined translation and rotation oscillations depends on five independent parameters. The equations of the forcing motions are defined as:

$$y(t) = A_t \sin(2\pi f_t t), \tag{1}$$

$$\theta(t) = A_\theta \sin(2\pi f_\theta t + \Phi), \tag{2}$$

where A_t (A_θ) is the amplitude of translational (rotational) motion, f_t (f_θ) is the frequency of translational (rotational) oscillation, and Φ is the phase difference between rotational and translational motions ***(refer to Figure 1)***. The five independent parameters can be written as translational and rotational Keulegan-Carpenter numbers:

$$KC_{[t,\theta]} = \frac{U_{\max_{[t,\theta]}}}{f_{[t,\theta]} D} = \frac{2\pi A_{[t,\theta]}}{D} \tag{3}$$

and as the translational and rotational Stokes number:

$$\beta_{[t,\theta]} = \frac{f_{[t,\theta]} D^2}{\nu} \tag{4}$$

where D is the diameter of the cylinder, U_{maxt} ($U_{max\theta}$) is the maximum translational (rotational) velocity of the cylinder motion and ν is the kinematic viscosity of the fluid. A Reynolds number can also be defined as a combination of two of the above dimensionless parameters. The associated translational Reynolds number, Re_t, is then:

$$Re_t = \frac{U_{\max} D}{\nu} = KC_t \beta_t. \tag{5}$$

METHODS AND TECHNIQUES

Experimental setup

The experiments were conducted in the FLAIR free-surface closed-loop water channel at the Department of Mechanical and Aerospace Engineering, Monash University. The model used for these experiments was a ***rigid*** hollow carbon fibre circular cylinder with a length of 800mm and outer diameter of 20mm, giving an aspect ratio of 40. The cylinder was suspended vertically from an actuator that was controlled by a micro-stepping stepper motor. The cylinder was fitted with an end plate to reduce the end effects. The end plate was designed following recommendations by Stansby [15], and consisted of a circular plate with a diameter of 9D. The Cartesian coordinate system in use is defined such that the origin is located at the centre of the circular cylinder (at t = 0) at the window shown in Figure 1 with x, y and z representing the streamwise, transverse, and spanwise directions, respectively. ***The window is located at a depth of 620mm under the water surface.*** The cylinder was

also oscillated rotationally by using another high-resolution stepper motor. The stepper motors were controlled using a two-axis indexer and two high-resolution drivers (running at 50800 steps/rev). A pure sinusoidal profile, as defined in equations (1) and (2), was used throughout the experiments. During each set of experiments the fluid was *initially* at rest, i.e. quiescent flow. Special care was always taken to ensure the quiescency of the flow. Prior to each set of experiment a honeycomb device was used to break large-scale structures into small-scale, minimising the background noise. Typically, the amplitude of the background noise, measured with the norm of velocity magnitude, was kept below 1.41% of the U_{maxt}, for β = 45. Experiments were performed for a particular set of parameters which has been shown previously to be that of a swimming cylinder [2]: the frequency ratios were held the same $\beta_t = \beta_\theta = \beta$, the amplitude of rotational motion $A_\theta = 1$ radian and the phase difference between the two motions $\Phi = \pi$. With these values the associated translational and rotational Keulegan-Carpenter number are $KC_t = KC_\theta = \pi$. The nondimensional frequency chosen ranged from $45 < \beta < 200$, consequently the range of Re_t covered $141 < Re_t < 628$.

Experimental technique: particle image velocimetry (PIV)

The PIV technique was used to measure the flow fields around the combined oscillating circular cylinder. The PIV set-up, illustrated in Figure 1, was based on that originally described by Adrian [16]. For this purpose, the flow was seeded with spherical polyamide particles having a mean diameter of 20 μm and specific gravity of 1.016. In this system, the particles were illuminated using two miniature Nd:YAG laser sources. The planes of interest for these experiments were the *yz*- and *xy*-plane, being the spanwise and streamwise perpendicular to the cylinder planes respectively, as shown in Figure 1. Pairs of images were captured on a high resolution CCD camera system with a maximum resolution of 4008×2672 pixels. The camera was equipped with a 105mm lens and was triggered by a TTL-signal, which was delivered from the stepper motor. At a particular phase in the oscillation cycle, a number of image pairs over successive cycles were stored for further processing, ***producing phase-locked velocity fields.***

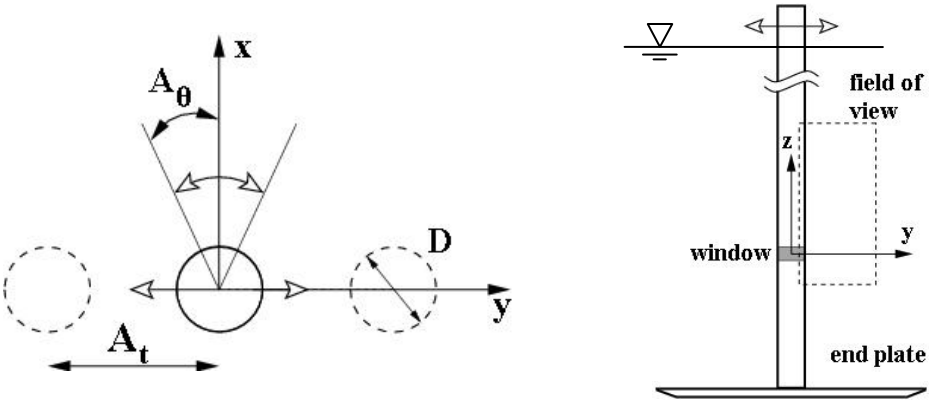

Figure 1. Schematic showing the problem geometry and important parameters relevant to the combined forced oscillation and the circular cylinder model. The green lines show the laser sheet in the streamwise plane (left) and spanwise plane (right).

Each image pair was processed using in-house PIV software ([17, 18]). This software uses a double-frame, cross-correlation multi-window algorithm to extract a grid of displacement vectors from the PIV images. An interrogation window of 32×32 (with an initial window size of 64×64) pixels was found to give satisfactory results with 50% overlap. More than 98% of the vectors were valid for all experiments. This window size corresponds to an average interrogation window of $0.064D \times 0.064D$ and measurement resolution of 249×166 (total of 41334) vectors in each field of view. The overall field of view was $8.0D \times 5.3D$. The displacement fields from these analyses are

presented using phase-averaged vorticity and velocity fields, where the phase-averages were calculated from 30 or more instantaneous velocity fields.

Numerical formulation

The base flows for the present study were calculated by solving the incompressible, time-dependent Navier-Stokes equations. The discretisation method employed was a spectral-element method, using seventh-order Lagrange polynomials associated with Gauss-Lobatto-Legendre quadrature points. A three-step time-splitting scheme is employed [19-21]. A computational domain extending $30D \times 30D$ was split into 518 elements, the majority of which were concentrated in the boundary layer. The resolution, element distribution and domain size are consistent with those used successfully in previous similar studies [20, 22 , 23]. At the cylinder surface, a time-dependent Dirichlet condition was utilized that varied sinusoidally in time according to the driven translational and rotational oscillation. The code employed a power method to resolve the most dominant Floquet mode (and the magnitude of the largest Floquet multiplier). Further details of the method in general can be found in [19], and details of the implementation used here in [20]; the formulation of Floquet stability analysis can also be found elsewhere [24].

RESULTS AND DISCUSSION

Figure 2 shows a comparison of the velocity at y/D=0.6 behind a purely translational oscillating circular cylinder in a quiescent flow. The measurements are taken at KC_t=5 and β=20, similar to previous numerical and experimental results of Dütsch et al. [8]. Figure 2 shows that the present experiment and the numerical simulations match the experimental results of Dütsch et al. [8] very closely. As can be seen, the present experimental results match more closely to the numerical results compared with the experimental results of Dütsch et al. [8]. Also excellent agreement was found with the results of Dütsch et al. [8] at different locations behind the cylinder which further validates our experimental setup.

Figure 3 shows the agreement between the present numerical simulation and the experiments for the ω_z vorticity contours around the cylinder undergoing combined translational and rotational oscillation at $KC=\Phi=\pi$ and $\beta=90$. On the left the present phase averaged experimental results are shown while on the right are the numerical simulations. The cylinder is at the middle of the oscillation cycle starting the motion towards the top of the page, in the vertical direction and rotating clockwise in the negative direction at the instant shown. These experiments confirm the earlier results of the numerical simulations of Blackburn et al. [2]. Figure 3 clearly shows the vorticity transport to one side of the cylinder as well as comparing the same flow between the present experimental and numerical investigation. Figure 3 also shows the excellent qualitative agreement between the experimental and numerical results.

Figure 4 shows the sequence of one complete cycle of translational and rotational oscillations in eight different consecutive snapshots, from t=0 to t=7T/8, where T is the period of oscillations. The cylinder, based on equations (1) and (2), starts the motion from the centre to the top of the page, the positive direction of y, and at the same time starts rotating clockwise, the negative direction of rotation angle, θ. Figure 4c shows the instant where the cylinder is at its maximum vertical position and the most negative angular displacement. As the oscillations are 180° out-of-phase, the maximum surface-tangential component of cylinder acceleration is located on the left hand side of the cylinder, i.e. it is where the accelerations are additive rather than in opposition. Morton [25] has shown that this combination of accelerations will result in the generation of vorticity on that side of the cylinder while the cancellation of accelerations on the other side results in a cross-annihilation of vorticity. The direction of rotation of the vortices will result in their being stretched and directed to only one side of the cylinder and perpendicular to its translation axis will necessarily result in thrust generation in this direction. Only in certain cases does the motion of the cylinder thus act to

produce vorticity more strongly from one side of the cylinder while retaining an overall zero production of vorticity from the cylinder. As reported by Blackburn at al. [2], for this to occur a threshold amplitude of oscillation is required. The phase angle between the motions seems to influence the degree to which cross-annihilation of vorticity occurs and the distance from the cylinder at which vorticity persists.

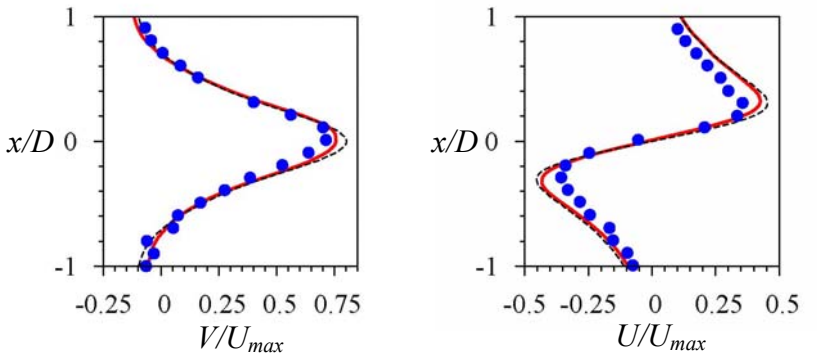

Figure 2. Comparison of the velocity components at y/D=0.6 behind the purely translationally oscillating cylinder in a quiescent flow (at KC_t=5 and β=20). solid (red) lines: present experiment; the dashed (black) lines: present numerical simulation; filled circle (blue) points: the experimental results of [8].

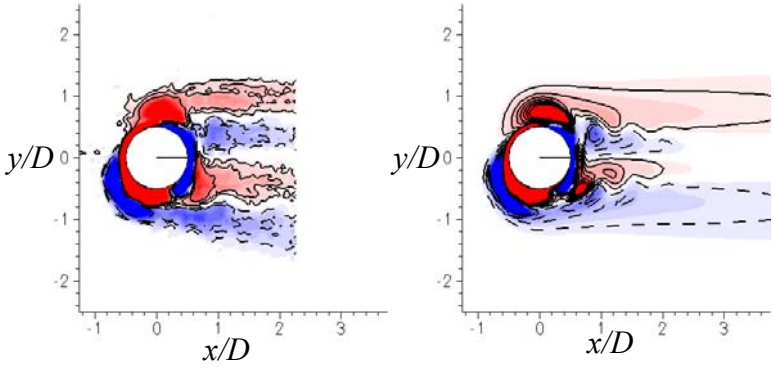

Figure 3. Vorticity contours, ω_z, around the cylinder undergoing combined translational and rotational oscillation at KC=Φ=π and β=90. The dashed lines (blue) are showing the clockwise direction of vorticities, negative, where the solid lines (red) are showing the counter-clockwise direction, positive. Left: present experiments; Right: numerical simulations.

Experiments were also undertaken to investigate the three-dimensional nature of the flow. The onset of three-dimensionality was measured and calculated to occur at β_c=32. Figure 5 shows the spanwise distribution of ω_x vorticity. Figure 5a shows the two-dimensionality of the flow for $\beta < \beta_c$ while at the higher β values shown in Figure 5b and c the flow displays a characteristic spanwise wavelength λ. The wavelength of the spanwise structures was found to be in the range $1.8 < \lambda/D < 2.0$. Numerical simulations with Floquet analysis have been performed and confirmed this wavelength; the comparison is shown in Figure 6.

CONCLUSIONS

The research reported here extends the study of Blackburn et al. [2] both experimentally and numerically. The study is restricted to the case with the phase angle set to Φ=π, and large amplitude oscillations-corresponding to a *swimming cylinder*. For the first time flow around a cylinder

undergoing a combined translation and rotation oscillatory motion has been measured experimentally. The development of wake three-dimensionality has also been examined experimentally. The stability of the wake to the growth of three-dimensional flow through Floquet stability analysis has also been determined. In particular, the experimental results along with our numerical simulations show and confirm how a cylinder at certain phase difference between the combined motions can generate thrust. Because of the phase difference, the oscillation velocities at the cylinder surface cancel on one side and reinforce on the other. This leads to preferential vorticity generation and transport on one side, and the cylinder rotational motion sweeps this vorticity around to the other side producing a thrust wake. We also find that the wake undergoes three-dimensional transition at low Reynolds numbers (Re ≈ 100) to an instability mode with a wavelength of about two cylinder diameters. The experimental results also indicate that the development of three-dimensionality in the wake leads to significant distortion of the previously two-dimensional wake.

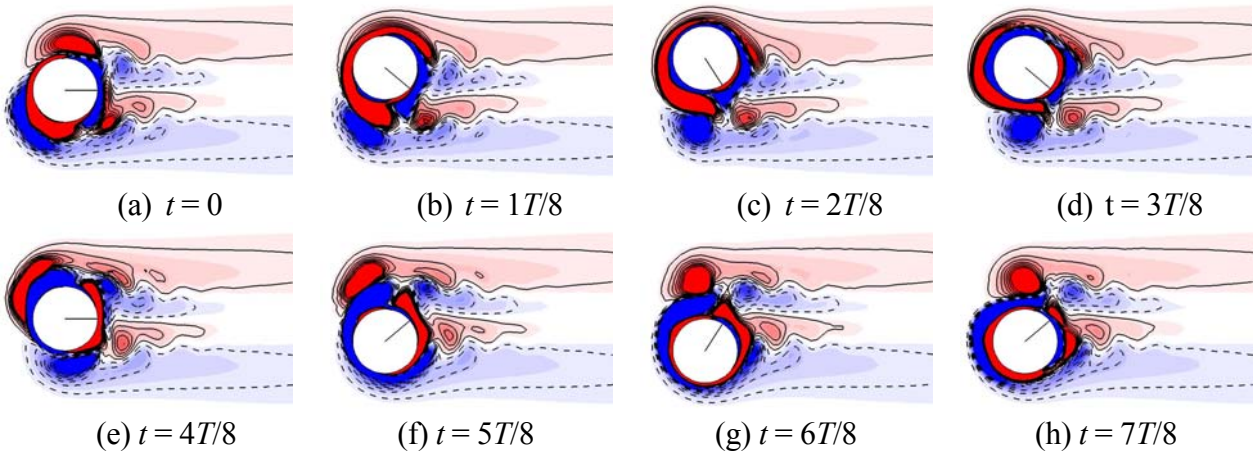

Figure 4. Flow produced by cylinder with combined oscillatory translation and rotation. This figure shows the sequence and development of the ω_z vorticity for one complete cycle, (a) $t = 0$ to (h) $t = 7T/8$ at $KC=\Phi=\pi$ and $\beta=90$ where T is the period of oscillation. The radial line shows the rotational displacement of the cylinder. The dashed lines (blue) are showing the clockwise direction of vorticities, negative, where the solid lines (red) are showing the counter clockwise direction, positive.

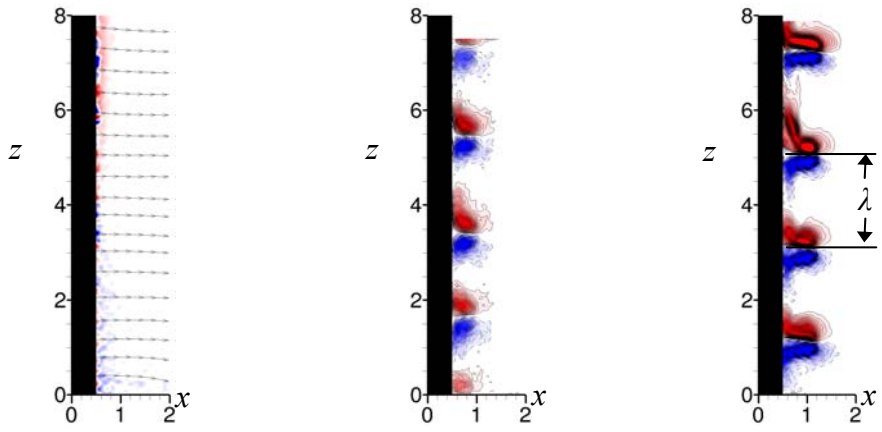

Figure 5. Spanwise distribution of flow for three values of β at $KC=\Phi=\pi$: (a) $\beta=20$: streamlines showing parallel and therefore two-dimensional vortex shedding; (b) and (c) β =45, 90, respectively: ω_x out-of-plane vorticity contours showing the mush-room structures along the span.

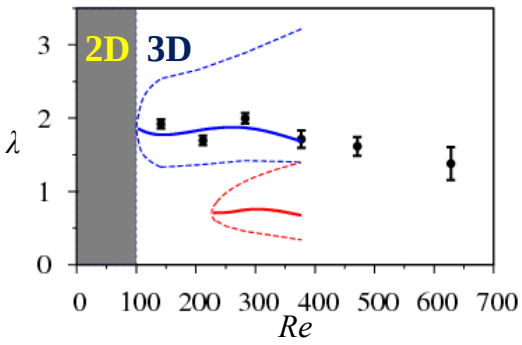

Figure 6. Comparison of the Floquet analysis predicted values for the wavelengths as a function of Reynolds number with experimental measurements for $KC=\Phi=\pi$.

ACKNOWLEDGEMENTS

MN would like to acknowledge the support of a Monash Graduate Scholarship (MGS) and a Monash International Postgraduate Research Scholarship (MIPRS). DLJ acknowledges support from ARC Discovery grant DP0774525 and computing time from the Australian Partnership for Advanced Computing (APAC).

REFERENCES

1. Bearman, P. W., Graham, J. M. R., Naylor, P., and Obasaju, E. D., *The role of vortices in oscillatory flow about bluff cylinders*, in *International Symposium on Hydrodynamics in Ocean Engineering*. 1981: Trondheim, Norway. p. 621-635.
2. Blackburn, H. M., Sheridan, J., and Elston, J. R., Bluff-body propulsion produced by combined rotary and translational oscillation. *Physics of Fluids*, Vol. 11, No.1, pp 4-6, 1999.
3. Honji, H., Streaked flow around an oscillating cylinder. *J. Fluid Mech.*, Vol. 107, pp 509-520, 1981.
4. Williamson, C. H. K., Sinusoidal flow relative to circular cylinders. *J. Fluid Mech.*, Vol. 155, pp 141-174, 1985.
5. Tatsuno, M. and Bearman, P. W., A visual study of the flow around an oscillating circular cylinder at low Keulegan-Carpenter numbers and low Stokes numbers. *J. Fluid Mech.*, Vol. 211, pp 157-182, 1990.
6. Justesen, P., A numerical study of oscillating flow around a circular cylinder. *J. Fluid Mech.*, Vol. 222, pp 157-196, 1991.
7. Iliadis, G. and Anagnostopoulos, G., Viscous oscillatory flow around a circular cylinder at low Keulegan-Carpenter numbers and frequency parameters. *International Journal for Numerical Methods in Fluids*, Vol. 26, pp 403-442, 1998.
8. Dütsch, H., Dusrt, F., Becker, S., and Lienhart, H., Low-Reynolds-number flow around an oscillating circular cylinder at low Keulegan-Carpenter numbers. *J. Fluid Mech.*, Vol. 360, pp 249-271, 1998.
9. Tokumaru, P. T. and Dimotakis, P. E., Rotary oscillation control of a cylinder wake. *J. Fluid Mech.*, Vol. 224, pp 77-90, 1991.
10. Poncet, P., Topological aspects of three-dimensional wakes behind rotary oscillating cylinders. *J. Fluid Mech.*, Vol. 517, pp 27-53, 2004.
11. Thiria, B., Goujon-Durand, S., and Wesfreid, J. E., The wake of a cylinder performing rotary oscillSations. *J. Fluid Mech.*, Vol. 560, pp 123-147, 2006.

12. Al-Mdallal, Q. M., Analysis and computation of the cross-flow past an oscillating cylinder with two degrees of freedom, Memorial University of Newfoundland Department of Mathematics and Statistics, 2004.
13. Lo Jacono, D., Nazarinia, M., Thompson, M. C., and Sheridan, J. Flow behind a cylinder forced by a combination of oscillatory translational and rotational motions. *Proceedings of XXII International Congress of Theoretical and Applied Mechanics*, Adelaide, Australia, University of Adelaide, August 24-29, 2008, pp 349.
14. Elston, J. R., The structures and instabilities of flow generated by an oscillating circular cylinder, *PhD Thesis*, Monash University Mech. Eng. Dept., Melbourne, 2005.
15. Stansby, P. K., The effect of end plates on the base pressure coefficient of a circular cylinder. *R. Aeronaut.*, Vol. 78, pp 36-37, 1974.
16. Adrian, R. J., Particle-imaging techniques for experimental fluid mechanics. *Annual Review Fluid Mechanics*, Vol. 23, pp 261-304, 1991.
17. Fouras, A., Lo Jacono, D., and Hourigan, K., Target-free stereo PIV: A novel technique with inherent error estimation and improved accuracy. *Experiments in Fluids*, Vol. 44, No.2, pp 317-329, 2008.
18. Fouras, A. and Soria, J., Accuracy of out-of-plane vorticity measurements derived from in-plane velocity field data. *Experiments in Fluids*, Vol. 25, pp 409-430, 1998.
19. Karniadakis, G. E. and Sherwin, S. J., *Spectral/hp methods for computational fluid dynamics*, Oxford Universoty Press, Oxford, 2005.
20. Thompson, M. C., Hourigan, K., and Sheridan, J., Three-dimensional instabilities in the wake of a circular cylinder. *Exp. Therm. Fluid Sci.*, Vol. 12, pp 190-196, 1996.
21. Canuto, C., Hussaini, M., Quarteroni, A., and Zang, T., *Spectral Methods in Fluid Dynamics*, Springer Verlag, 2nd ed, Berlin and New York, 1990.
22. Leontini, J. S., Thompson, M. C., and Hourigan, K., Three-dimensional transition in the wake of a transversely oscillating cylinder. *J. Fluid Mech.*, Vol. 577, pp 79-104, 2007.
23. Thompson, M. C., Leweke, T., and Williamson, C. H. K., The physical mechanism of transition in bluff body wakes. *J. Fluids & Structures*, Vol. 15, pp 607-616, 2001.
24. Barkley, D. and Henderson, R. D., Three-dimensional Floquet stability analysis of the wake of a circular cylinder. *J. Fluid Mech.*, Vol. 322, pp 215-241, 1996.
25. Morton, B. R., The generation and decay of vorticity. *Geophysical & Astrophysical Fluid Dynamics*, Vol. 28, No.3, pp 277-308, 1984.